Proceedings of the 17th World Congress
The International Federation of Automatic Control
Seoul, Korea, July 6-11, 2008

Implementation of Linear Homing Guidance Law on a Two-Part Homing Missile

Bülent Özkan*. M. Kemal Özgören.**
Gökmen Mahmutyazıcıoğlu***

** The Scientific and Technological Research Council of Turkey, Defence Industry Research and Development Institute, Ankara, Turkey (e-mail: bozkan@sage.tubitak.gov.tr)*
*** Middle East Technical University, Mechanical Engineering Department,, Ankara, Turkey, (e-mail: ozgoren@metu.edu.tr)*
**** The Scientific and Technological Research Council of Turkey, Defence Industry Research and Development Institute, Ankara, Turkey (e-mail: gmahmut@sage.tubitak.gov.tr)*

Abstract: Because of its simplicity and ease of implementation, the proportional navigation guidance (PNG) law is chosen in most of the guidance applications. In this study, the linear homing guidance (LHG) law is proposed as an alternative to PNG and its implementation on a two-part missile against a moving surface target is presented. First, the missile dynamics is modeled. Afterwards, the formulation of LHG is given. Modeling the target kinematics as well, the entire guidance and control system is built by integrating all the models mentioned above, and the relevant computer simulations are carried out. Consequently, the simulation results obtained with LHG are compared to the data acquired from the simulations with PNG. The simulations also involve the sensitivity analysis and design of modified autopilots with varying-bandwidth values upon the implementation of LHG. Finally, all the results are evaluated.

1. INTRODUCTION

After the World War II, guided missiles have become one of the popular munitions in the military field because they have the ability of hitting the intended target precisely. In order to increase the lethality of the missiles, several guidance methods have been proposed by the engineers and scientists working in this field (Özkan, 2005, Shinar, 1973, and Vermishev, 1969). While some of these methods consider missile-target engagement problems against stationary or slowly moving targets, the ones developed in recent years deal with the guidance of the homing missiles toward manoeuvring targets (Han *et al*., 2002, Lin *et al.*, 1999, Menon *et al*., 2003, and Zarchan, 1994 and 1998). Among all these methods, the proportional navigation guidance (PNG) law has become the most popular guidance law because of its simplicity and ease in implementation (Adler, 1956, Gurfil *et al*., 2001, Lin, 1991, Mahmutyazıcıoğlu, 1994, and Zarchan, 1994). On the other hand, it is seen that the effectiveness of PNG decreases as the manoeuvre level of the intended target is increased.

In this work, the linear homing guidance (LHG) law is proposed as an alternative to the PNG law especially against manoeuvring targets. The entire guidance and control model is built for a two-part missile configuration and the performance of the LHG on this missile is evaluated according to the final miss distances of the missile from the target, missile-target engagement time, maximum acceleration requirement of the missile, and total energy consumption. The initial heading error of the missile, target manoeuvre, dynamics of the guidance and control system, acceleration limit of the missile, mechanical limit of the aerodynamic control fins, and other external effects are added to the guidance and control model as the error sources affecting the success of the missile. After the relevant computer simulations, the attained results are compared to those found with the PNG law and the suggestions for the amendment of the performance of the LHG law are made (Özkan, 2005, and Özkan *et al*., 2007).

2. MISSILE MODEL

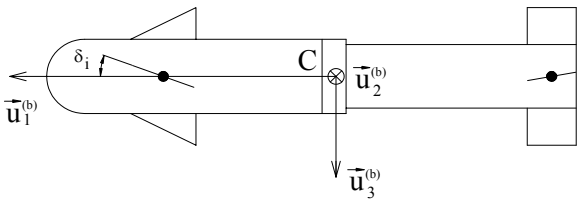

Fig. 1. Missile model

In this study, an aerodynamically-controlled canard-type missile consisting of two-bodies that are connected to each other by means of a roller bearing is dealt with. The tail fins of the missile are taken to be uncanted. The equations of motion of the missile whose schematic representation is given in Fig. 1 can be obtained by applying the Newton-Euler force and

moment equalities with respect to the body-fixed frame of the entire missile (F_b) as given below:

$$\dot{u} - r\,v + q\,w = \left(X + X_T\right)/m + g_x \quad (1)$$

$$\dot{v} + r\,u - p\,w = \left(Y + Y_T\right)/m + g_y \quad (2)$$

$$\dot{w} - q\,u + p\,v = \left(Z + Z_T\right)/m + g_z \quad (3)$$

$$\dot{p} = \left(L_1 + b_t\,\dot{\phi}_s\right)/I_{a1} \quad (4)$$

$$\dot{p}_2 = \left(L_2 + L_T - b_t\,\dot{\phi}_s\right)/I_{a2} \quad (5)$$

$$\dot{q} - p\,r\left(1-\mu\right) + p_2\,r\,\kappa = \left(M + M_T - \lambda\,Z_T\right)/I_t \quad (6)$$

$$\dot{r} + p\,q\left(1-\mu\right) - p_2\,q\,\kappa = \left(N + N_T + \lambda\,Y_T\right)/I_t \quad (7)$$

As $\mu = m_1/m_2$ and $\kappa = I_{a2}/I_t$, the parameters in equations (1) through (7) are defined as follows.

m, m_1, and m_2: Masses of the entire missile, front part, and rear part

I_a and I_t: Axial and lateral moment of inertia components

b_t: Viscous friction coefficient of the roller bearing

λ: Distance between the mass centres of the entire missile and rear part

ϕ_s: Spin angle of the rear body about $\vec{u}_1^{(b)}$ axis

p, q, and *r*: Angular velocity components in the roll, pitch, and yaw directions

u, v, and *w*: Linear velocity components

X, Y, and *Z*: Aerodynamic force components acting on the missile at its mass centre (point C)

L_1 and L_2: Roll components of the aerodynamic moments acting on the front and rear parts

M and *N*: Pitch and yaw components of the aerodynamic moments acting on the missile body

X_T, Y_T, and Z_T: Thrust force components on the missile at its mass centre

L_T, M_T, and N_T: Thrust misalignment moment components

g_x, g_y, and g_z: Gravity components acting on the missile at its mass centre

Regarding the roll motion of the missile, it is compensated by means of a roll autopilot prior to the motions in the pitch and yaw directions, i.e. $p \approx 0$, the equations of motion of the missile in the pitch and yaw planes after the end of thrust can be written using equations (2), (3), (6), and (7) as follows:

$$\dot{w} - q\,u = \left(Z/m\right) + g_z \quad (8)$$

$$\dot{q} = M/I_t \quad (9)$$

$$\dot{v} + r\,u = \left(Y/m\right) + g_y \quad (10)$$

$$\dot{r} = N/I_t \quad (11)$$

Since the engagement problem is handled in the terminal guidance phase, the missile is lack of thrust effect. Thus, its thrust model is not given here.

3. AERODYNAMIC MODEL

The aerodynamic force and moment components in equations (8) through (11), i.e. Y, Z, M, and N, can be expressed in the following manner:

$$Y = C_y\,q_\infty\,S_M \quad (12)$$

$$Z = C_z\,q_\infty\,S_M \quad (13)$$

$$M = C_m\,q_\infty\,S_M\,d_M \quad (14)$$

$$N = C_n\,q_\infty\,S_M\,d_M \quad (15)$$

In equations (12) through (15), $q_\infty, S_M,$ *and* d_M stand for the dynamic pressure on the missile, missile cross-sectional area, and missile diameter, respectively. Regarding the considered missile geometry, the aerodynamic coefficients, i.e. C_y, C_z, C_m, and C_n, are computed for the Mach number, i.e. M_∞, in the range of 0.3 through 2.7, elevator and rudder deflections, i.e. δ_e and δ_r, in the range of -10 through 10°, and angle of attack and side-slip angle, i.e. α and β, in the range of -17 through 19°. Here, C_y, C_z, C_m, and C_n coefficients can be written as the functions of α, β, δ_e, δ_r, q, and r as given below:

$$C_y = C_{y_\beta}\,\beta + C_{y_\delta}\,\delta_r + C_{y_r}\,r\left[d_M/\left(2v_M\right)\right] \quad (16)$$

$$C_z = C_{z_\alpha}\,\alpha + C_{z_\delta}\,\delta_e + C_{z_q}\,q\left[d_M/\left(2v_M\right)\right] \quad (17)$$

$$C_m = C_{m_\alpha}\,\alpha + C_{m_\delta}\,\delta_e + C_{m_q}\,q\left[d_M/\left(2v_M\right)\right] \quad (18)$$

$$C_n = C_{n_\beta}\,\beta + C_{n_\delta}\,\delta_r + C_{n_r}\,r\left[d_M/\left(2v_M\right)\right] \quad (19)$$

In equations (16) through (19), v_M denotes the magnitude of the missile velocity vector. The stability derivatives represented by C_{y_β}, C_{y_δ}, C_{y_r}, C_{z_α}, C_{z_δ}, C_{z_q}, C_{m_α}, C_{m_δ}, C_{m_q}, C_{n_β}, C_{n_δ}, and C_{n_r} are functions of M_∞ and they are continuously updated depending on the present values of the related flight parameters during the computer simulations.

4. GUIDANCE METHOD

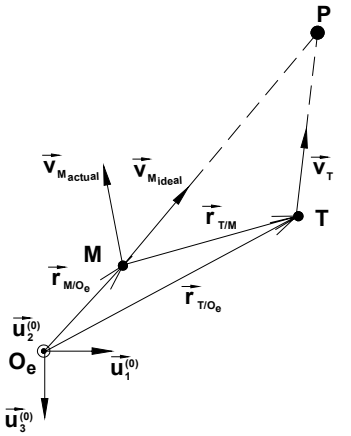

Fig. 2. Linear homing guidance law geometry

In this study, the LHG law is used for the terminal guidance phase of the designated interception problem. Here, the terminal guidance phase is defined as the duration from the instant at which the seeker detects the target to the end of the missile-target

engagement. Also, the PNG law with the effective navigation ratio of three is considered for comparison purposes (Özkan, 2005).

In this approach, it is intended to keep the missile always on the collision triangle that is formed by the missile, the target, and the predicted intercept point. For this purpose, the most appropriate way is to orient the missile velocity vector toward the predicted intercept point at which the missile-target collision will occur after a while as depicted in Fig. 2. Then, the resulting guidance commands will be in the form of the flight path angles of the missile (Özkan *et al.*, 2007).

In Fig. 2, O_e denotes the origin of the Earth-fixed frame; M, T, and P stand for the missile, the target, and the predicted intercept point, and $\vec{v}_{Mactual}$ and $\vec{v}_{Mideal}$ show the velocity vector of the missile at the beginning of the guidance and ideal velocity vector, respectively. The velocity vector of the missile in order to be on the collision triangle is then indicated by $\vec{v}_{Mideal}$.

Using the LHG law, the command angles for the pitch and yaw planes, i.e. γ_m^c and η_m^c, can be generated as follows (Özkan, 2005):

$$\gamma_m^c = arctan\left(\frac{\Delta z - v_{Tz}\,\Delta t}{\varsigma_x\ cos(\eta_m) + \varsigma_y\ sin(\eta_m)}\right) \qquad (20)$$

$$\eta_m^c = arctan\left[\left(v_{Ty}\,\Delta t - \Delta y\right)/\left(v_{Tx}\,\Delta t - \Delta x\right)\right] \qquad (21)$$

Here, for i=x, y, z and j=M, T; $\varsigma_x = v_{Tx}\,\Delta t - \Delta x$, $\varsigma_y = v_{Ty}\,\Delta t - \Delta y$, and $\Delta i = i_M - i_T$ as x, y, and z show the position components on the Earth-fixed frame. Also, v_{Tx} and v_{Ty} represent the components of the target velocity and Δt denotes the duration required for the missile to attain the predicted intercept point from its current position, and is a function of the position and velocity components of the missile and target.

5. MISSILE CONTROL SYSTEM

In order to convert the angle commands produced by the LHG law into physical motions, an angle control system is constructed based on the state-feedback algorithm. In this control system, the integral of the error between the flight path angle command and actual flight path angle value, i.e. x_i, is assigned as the additional state variable. As similar to that in the yaw plane, the angle control system in the pitch plane is given by the block diagram in Fig. 3.

In this model, the dynamics of the gyroscopes and accelerometers are neglected because their operating frequency values are very high (around 110 Hz) compared to the missile control system bandwidth assigned to be 5 Hz. The bandwidth of the control actuation system is selected to be 20 Hz such that it does not affect the control system dynamics. Also, the motions of the control fins are limited by ±20°.

In the computer simulations, the autopilot gains are continuously updated depending on the current value of the dynamic pressure. In order to get the corresponding autopilot gains, the closed-loop transfer functions derived from the linearized pitch and yaw plane equations of motion are determined in the following manner:

$$\frac{\gamma_m(s)}{\gamma_{md}(s)} = \frac{n_{\gamma 3}\,s^3 + n_{\gamma 2}\,s^2 + n_{\gamma 1}\,s + 1}{d_{\gamma 4}\,s^4 + d_{\gamma 3}\,s^3 + d_{\gamma 2}\,s^2 + d_{\gamma 1}\,s + 1} \qquad (22)$$

$$\frac{\eta_m(s)}{\eta_{md}(s)} = \frac{n_{\eta 3}\,s^3 + n_{\eta 2}\,s^2 + n_{\eta 1}\,s + 1}{d_{\eta 4}\,s^4 + d_{\eta 3}\,s^3 + d_{\eta 2}\,s^2 + d_{\eta 1}\,s + 1} \qquad (23)$$

In equations (22) and (23), as $\gamma_{md} = \gamma_m^c$ and $\eta_{md} = \eta_m^c$, the pre-multiplier coefficients of s parameter which is the Laplace operator are functions of the diameter, mass, moment of inertia, and velocity components of the missile as well as the autopilot gains, dynamic pressure, and aerodynamic coefficients.

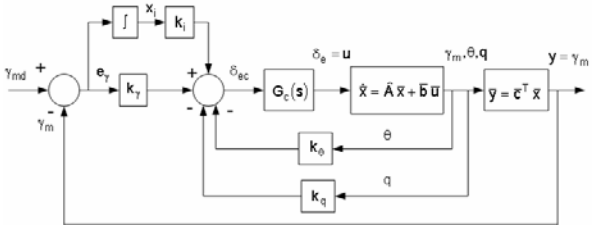

Fig. 3. Angle autopilot for the pitch plane

The autopilot gains are obtained by equating a fourth-order Butterworth polynomial to the characteristic polynomial of each transfer function in equations (22) and (23) in order to make the missile control system stable and to reach the desired bandwidth value, i.e. 5 Hz (Özkan, 2005).

6. TARGET KINEMATICS

Specifying the normal and tangential acceleration components, i.e. a_T^n and a_T^t, in addition to the initial values of the velocity and flight path angle, i.e. v_{T0} and γ_{t0}, the velocity and flight path angle of the target (v_T and η_t) can be expressed depending on time as follows:

$$v_T(t) = v_{T0} + \int_{t_0}^{t} a_T^t(\tau)\,d\tau \qquad (24)$$

$$\eta_t(t) = \eta_{t0} + \int_{t_0}^{t} \left[a_T^n(\tau)/v_T(\tau)\right] d\tau \qquad (25)$$

In equations (24) and (25), t_0 and τ denote the initiation of the missile-target engagement and dummy integration variable, respectively.

Taking the time integrals of equations (24) and (25), the expressions giving the change of the target position with respect to time can be determined for the specified initial values of the target position in the

horizontal plane, i.e. x_{T0} and y_{T0}. Since a surface target is concerned in this study, the elevation of the target is taken to be constant, i.e. $z_T(t) = z_{T0}$.

$$x_T(t) = x_{T0} + \int_{t_0}^{t} v_T(\tau)\, cos(\eta_t(\tau))\, d\tau \quad (26)$$

$$y_T(t) = y_{T0} + \int_{t_0}^{t} v_T(\tau)\, sin(\eta_t(\tau))\, d\tau \quad (27)$$

7. MISSILE-TARGET ENGAGEMENT MODEL

The relative distance between the missile and target, i.e. $r_{T/M}$, and the line-of-sight angles defined as the angles from $r_{T/M}$ to the pitch and yaw planes, i.e. λ_y and λ_p, can be written in the following fashion:

$$r_{T/M} = \left(\Delta x^2 + \Delta y^2 + \Delta z^2\right)^{1/2} \quad (28)$$

$$\lambda_y = arctan(\Delta y / \Delta x) \quad (29)$$

$$\lambda_p = arctan\left(-\Delta z\, cos(\lambda_y) / \Delta x\right) \quad (30)$$

In the simulations, a strapdown, or body-fixed, seeker model with the field-of-view of ±50° is used (Özkan, 2005).

Since a surface target is considered in the study, the total miss distance at the end of the missile-target engagement, i.e. d_{miss} at $t = t_F$ can be calculated from the following formula just as the vertical component of $r_{T/M}$ becomes zero, i.e. $\Delta z = 0$.

$$d_{miss} = \left(\Delta x^2(t_F) + \Delta y^2(t_F)\right)^{1/2} \quad (31)$$

8. COMPUTER SIMULATIONS

Using the entire guidance and control model, the performance of the LHG law is evaluated for the missile initial heading errors of 0 and -20° and target lateral acceleration level of 0 and 0.5g ($g = 9.81\ m/s^2$). The terminal miss distance, engagement time, maximum acceleration requirement, and total energy consumption are chosen as the performance criteria. In this extent, it is assumed that the target has a motion of constant velocity, i.e. the motion with zero tangential acceleration component, and hence only the normal, or lateral, acceleration component of the target is taken into account.

The simulation results are presented in Table 1. In this table, the results obtained with the PNG law with the effective navigation ratio of three in both of the pitch and yaw planes are also given. In the simulations, the lateral acceleration limit the missile can endure is taken to be ±30g. All the computer simulations were carried out in the Matlab Simulink environment.

To compare with the PNG law, the sensitivity of the LHG law to the information of the target position components is examined. In this extent, first the case at which both the heading error and lateral acceleration of the target are zero is taken into account. Afterwards, the lateral acceleration of the target is set to 0.5g while the heading error remains zero. The relevant results are given in Table 2 and Table 3.

Table 1. Simulation results for the LHG and PNG laws

Initial Heading Error (°)	Target Lateral Acceleration (g)	Guidance Law	Terminal Miss Distance (m)	Missile-Target Engagement Time (s)	Maximum Acceleration Requirement (g)	Total Energy Consumption (kJ)
0	0	LHG	2.435	3.052	57.154	2.755
		PNG	4.840	3.047	2.951	12.257
0	0.5	LHG	3.430	3.039	57.154	2.699
		PNG	4.632	3.038	3.084	13.415
-20	0	LHG	3.205	3.049	942.95	172.717
		PNG	5.578	3.288	16.528	217.395
-20	0.5	LHG	3.325	3.039	942.95	172.852
		PNG	5.597	3.306	16.528	239.068

Table 2. Simulation results for the target parameter uncertainties for zero heading error and lateral acceleration of the target

Amount of Uncertainty in Target Position (%)	Amount of Uncertainty in Target Velocity (%)	Terminal Miss Distance (m)	Engagement Time (s)	Maximum Acceleration (g)	Total Energy Consumption (kJ)
0	0	2.435	3.052	57.154	2.755
1	0	18.448	3.120	65.207	2.978
-5	0	111.411	2.710	89.367	4.399
0	1	3.126	3.050	57.649	2.950
0	-5	2.868	3.050	55.657	2.897
0	-20	3.955	3.047	50.677	2.776
0	-50	4.276	3.046	40.717	2.576
0	-100 (v_T=0)	5.695	3.041	24.115	2.286

Table 3. Simulation results for the target parameter uncertainties for zero heading error and 0.5 g of lateral acceleration of the target

Amount of Uncertainty in Target Position (%)	Amount of Uncertainty in Target Velocity (%)	Terminal Miss Distance (m)	Engagement Time (s)	Maximum Acceleration (g)	Total Energy Consumption (kJ)
0	0	3.430	3.039	57.154	2.699
-1	0	25.024	2.970	53.403	2.813
0	-5	3.722	3.038	55.657	2.888
0	-10	3.238	3.040	53.997	2.856
0	-100 (v_T=0)	4.744	3.036	24.115	2.319

As seen from the tables above, the most important drawback of the LHG law is the amount of the maximum acceleration demand. In fact, these values occur at the beginning of the engagement because the LHG law tries to put the velocity vector of the missile on the collision triangle as soon as possible. If this value can be lowered, the LHG law will be very competitive to PNG. In order to decrease the amount of the maximum lateral acceleration components, the most widely-used way is to limit the guidance commands by filtering them. As an alternative to this approach, the bandwidths of the yaw and the pitch autopilots can be adjusted as a function of time as given below:

$$f_c(t)=\begin{cases} a\cdot t+b & ,\quad for\ t_0 \le t < t_E \\ f_c(t_E) & ,\quad for\ t \ge t_E \end{cases} \qquad (32)$$

where, for t_0, t_E, and $f_c(t)$ stand for the initial time of the engagement, end of the duration of the varying bandwidth, and bandwidth as a function of time, and for $\Delta t = t_0 - t_E$, $a=\left[f_c(t_0)-f_c(t_E)\right]/\Delta t$ and $b=\left[f_c(t_E)t_0 - f_c(t_0)t_E\right]/\Delta t$.

Table 4. Simulation results with varying-bandwidth autopilots for t_E=0.5 s

Initial Heading Error (°)	Target Lateral Acceleration (g)	Terminal Miss Distance (m)	Missile-Target Engagement Time (s)	Maximum Acceleration Requirement (g)	Total Energy Consumption (kJ)
0	0	4.640	3.043	9.351	2.363
0	0.5	4.224	3.035	9.063	2.348
-20	0	3.034	3.054	80.660	20.981
-20	0.5	4.874	3.038	81.317	20.868

Table 5. Simulation results with varying-bandwidth autopilots for t_E=1 s

Initial Heading Error (°)	Target Lateral Acceleration (g)	Terminal Miss Distance (m)	Missile-Target Engagement Time (s)	Maximum Acceleration Requirement (g)	Total Energy Consumption (kJ)
0	0	2.997	3.049	6.193	2.349
0	0.5	2.473	3.041	6.251	2.323
-20	0	3.224	3.057	65.611	25.689
-20	0.5	2.648	3.049	66.132	25.183

Choosing $t_0 = 0,\ f_c(t_0) = 1\ Hz\ and\ f_c(t_E) = 5\ Hz$, the results in Table 4 and Table 5 are determined for $t_E = 0.5\ s$ and $t_E = 1\ s$. The changes of the resultant command accelerations are shown in Fig. 4 and Fig. 5 for both t_E values considering zero heading error of the missile and 0.5g of lateral acceleration of the target. The existing angular velocity components of the missile within the first second of the planned engagement are also given in Fig. 6.

As shown from Fig. 4 and Fig. 5, the acceleration demand has an oscillatory behaviour within the region in which the bandwidth values of the yaw and pitch autopilots vary in time. Since the missile velocity vector is tried to be put on the collision triangle as soon as possible and because of the varying characteristics of the autopilot bandwidths, these oscillations come into the picture. Moreover, as the amount of t_E becomes larger, the maximum value of the command acceleration also grows up.

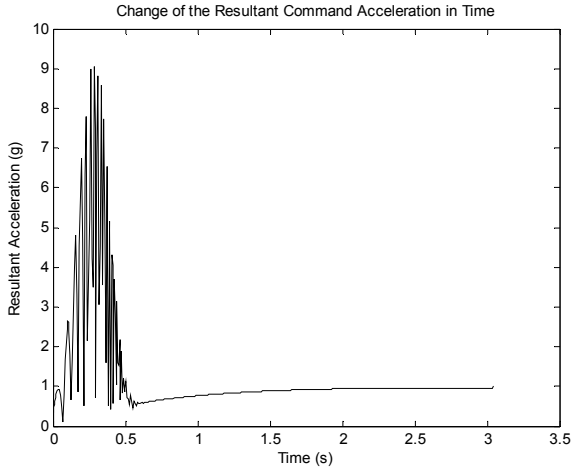

Fig 4. Change of the command acceleration, t_E=0.5 s

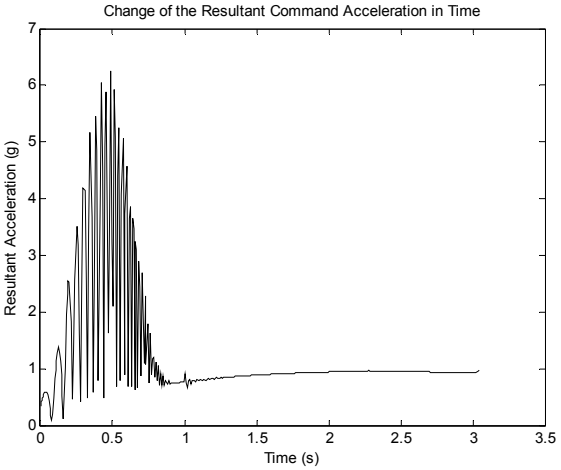

Fig 5. Change of the command acceleration, t_E=1 s

9. CONCLUSIONS

Looking at Table 1, the LHG law yields the smaller values than the PNG law in terms of the terminal miss distance and total energy consumption. The missile-target engagement times are nearly equal for the same scenarios. On the other hand, the maximum acceleration requirement of the original LHG law is much higher than that of the PNG law because of the fact that the initial lateral acceleration demand of the LHG law necessary to put the velocity vector of the missile on the collision triangle is quite large. Actually, one of the remedies to overcome this problem is to design the missile autopilots for the pitch and yaw planes with varying bandwidths as explained above.

Furthermore, when Table 2 and Table 3 are carefully examined, it is seen that the success of the LHG law is strongly dependent on the measurement of the target position. On the other hand, the measurement accuracy of the target velocity does not affect the results much more. In fact, this is because the target speed is much smaller than the missile speed for the considered target. Conversely, regarding an air target whose speed is much greater than a surface target, it is expected for the results to be more sensitive to the measurement accuracy of the target velocity.

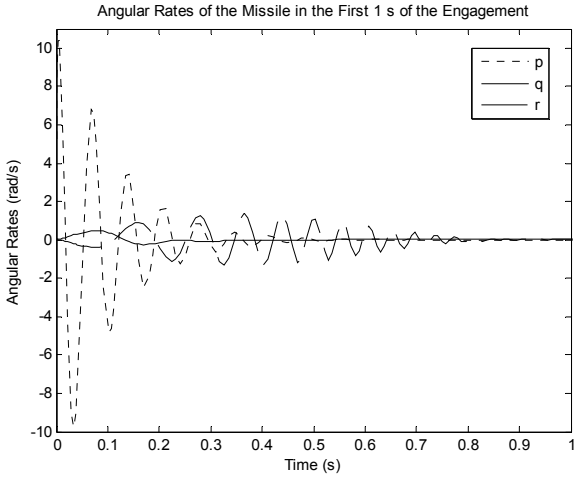

Fig 6. Angular velocity components for t_E=1 s

As seen from Table 4 and Table 5 which reflect the results of the computer simulations with varying-bandwidth autopilots, the maximum command acceleration and the total energy consumption values are very smaller than those in the case of the constant-bandwidth autopilots while the terminal miss distance becomes larger. Also, the engagement time values are slightly greater. Comparing the results obtained for t_E=*0.5 s* and t_E=*1 s*, the terminal miss distance and the maximum acceleration values happen to be smaller as t_E is enlarged. This is because the duration to put the missile velocity vector on the collision triangle is increased from 0.5 to 1 s. Thus, this leads the amount of the maximum acceleration demand of the missile and hence the final miss distance to become smaller. On the other hand, since the time to attain the specified constant autopilot bandwidth gets longer, the engagement time happens to be larger. Moreover, as t_E values is increased, the total energy consumption value decreases for zero initial heading errors while it tends to grow for the cases with nonzero initial heading error values.

Eventually, it can be concluded that the LHG law gives better results than the PNG law in terms of the considered performance criteria except the maximum acceleration requirement. Also, designing the pitch and yaw autopilots of the missile with varying bandwidths, the acceleration requirement of the LHG law becomes much smaller. Yet, the PNG law is still better than the LHG law in this sense.

REFERENCES

Adler, F. (1956), Missile Guidance by Three-Dimensional Proportional Navigation, *Journal of Applied Physics*, **Vol. 27, No. 5**, pp. 500-507.

Gurfil, P., Jodorkovsky, M., and Guelman, M. (2001), Neoclassical Guidance for Homing Missiles, *Journal of Guidance, Control and Dynamics,* **Vol: 24, No: 3**, pp. 452-459.

Han, D., Balakrishnan, S. N., and Ohlmeyer, E. J. (2002), Optimal Midcourse Guidance Law with Neural Networks, *Proceedings of the IFAC 15th Triennial World Congress*, Barcelona, Spain.

Lin, C. F. (1991), *Modern Navigation, Guidance and Control Processing*, Prentice Hall Publication, Englewood Cliffs, New Jersey.

Lin, C. L. and Chen, Y. Y. (1999), Design of Advanced Guidance Law against High Speed Attacking Target, *Proceeding of National Science Council*, ROC(A), **Vol. 23, No. 1**, pp. 60-74.

Mahmutyazıcıoğlu, G. (1994), *Dynamics and Control Simulation of an Inertially Guided Missile*, M.Sc. Thesis, Middle East Technical University, Turkey

Menon, P. K., Sweriduk, G. D., and Ohlmeyer, E. J. (2003). Optimal Fixed-Interval Integrated Guidance-Control Laws for Hit-to-Kill Missiles, *AIAA Guidance, Navigation and Control Conference*, Austin, USA.

Özkan, B. (2005). *Dynamic Modeling, Guidance, and Control of Homing Missiles*, Ph.D. Thesis, Middle East Technical University, Ankara, Turkey.

Özkan, B., Özgören, M.K., and Mahmutyazıcıoğlu, G. (2007). Comparison of the Linear Homing, Parabolic Homing, and Proportional Navigation Guidance Methods on a Two-Part Homing Missile against a Surface Target, *2nd European Conference for Aerospace Sciences (EUCASS)*, Brussels, Belgium.

Shinar, J. (1973), Homing of Rolling Missile against a Manoeuvering Target, *Israel Journal of Technology*, **Vol. 11, No. 3**, pp. 117-130.

Vermishev, Y. K. (1969), *Fundamentals of Missile Guidance*, Translation Division Foreign Technology Division.

Zarchan, P. (1998), Ballistic Missile Defense Guidance and Control Issues, *Science and Global Security*, **Vol. 8**, pp. 99-124.

Zarchan, P. (1994). *Tactical and Strategic Missile Guidance*, Second Edition, Progress in Astronautics and Aeronautics, USA.